Hydrol. Earth Syst. Sci. Discuss., 11, 5831–5857, 2014
www.hydrol-earth-syst-sci-discuss.net/11/5831/2014/
doi:10.5194/hessd-11-5831-2014

Hydrology and Earth System Sciences Discussions
Open Access

Transferring the concept of minimum energy expenditure from river networks to subsurface flow patterns

S. Hergarten[1], **G. Winker**[2], **and S. Birk**[2]

[1]Institut für Geo- und Umweltnaturwissenschaften, Albertstr. 23B, 79104 Freiburg, Germany
[2]Institut für Erdwissenschaften, Karl-Franzens-Universität Graz, Heinrichstraße 26, 8010 Graz, Austria

Received: 29 April 2014 – Accepted: 23 May 2014 – Published: 4 June 2014

Correspondence to: S. Hergarten (stefan.hergarten@geologie.uni-freiburg.de)

Published by Copernicus Publications on behalf of the European Geosciences Union.

Abstract

Principles of optimality provide an interesting alternative to modeling hydrological processes in detail on small scales. However, the concepts still seem to be on a visionary level except for the theory of minimum energy expenditure for river networks. Inspired by this approach, we present a theory of minimum energy expenditure in subsurface flow in order to obtain a better understanding of preferential flow patterns in the subsurface. The concept describes flow patterns which are optimal in the sense that they minimize the total energy expenditure at given recharge under the side condition of a given total porosity. Results are illustrated using two examples: two-dimensional flow towards a spring with a radial symmetric distribution of the porosity and dendritic flow patterns. The latter are found to be similar to river networks in their structure and, as a main result, the model predicts a power-law distribution of the spring discharges. In combination with two data sets from the Austrian Alps, this result is used for validating the model. Both data sets reveal power-law distributed spring discharges with similar scaling exponents. These are, however, slightly larger than the exponent predicted by the model. As a further result, the distributions of the residence times strongly differ between homogeneous porous media and optimized flow patterns, while the mean residence times seem to be similar in both cases.

1 Introduction

Preferential flow due to heterogeneity is one of the most important topics in subsurface hydrology. In many cases, large parts of the uncertainty in modeling subsurface flow and transport arises from preferential flow patterns which are either not known in detail or too small-scaled to be included explicitly in the model.

Preferential flow patterns may be the result of external pre-design, but may also be created by the flow itself. Fractured aquifers and reservoirs mainly fall into the first category. Fractures may be opened at high fluid pressures (hydraulic fracturing,

HESSD
11, 5831–5857, 2014

fluid-induced seismicity), but the basic structure of the preferential flow pattern is still governed by the geologic pre-design here. In contrast, the role of pre-design is less clear for preferential flow in soils and in karstified aquifers. In particular, the formation of conduit patterns in karst has been addressed by several modeling studies (e.g. Groves and Howard, 1994; Howard and Groves, 1995; Siemers and Dreybrodt, 1998; Kaufmann and Braun, 1999; Kaufmann and Braun, 2000; Liedl et al., 2003; Dreybrodt et al., 2005; Kaufmann et al., 2010; Gabrovšek and Dreybrodt, 2011; Hubinger and Birk, 2011), pioneered by early work of Kiraly (1979). Although there may be some pre-design, too, it is generally believed that the solution of material by the flow causes a strong tendency towards self-organization of the flow pattern.

The idea to derive self-organizing heterogeneity by principles of optimality instead of small-scale, physically-based models has received growing interest in the last years (McDonnell et al., 2007; Kleidon and Schymanski, 2008). The idea to explain the morphology of river networks from the principle of minimum energy expenditure even dates back to the early 1990s (Rodriguez-Iturbe et al., 1992a, b; Rinaldo et al., 1992) and turned out to be rather successful, although this concept could never been strictly derived from physical laws.

Beside the application to river networks, the concept of maximum entropy production (MEP) (e.g. Kleidon and Schymanski, 2008) is widely considered in hydrology. It is obviously inspired by the second thermodynamic law, stating that entropy cannot be consumed but only produced. The concept of MEP now assumes that open systems in a steady state organize towards a state of maximum production of entropy. However, it should be clearly stated that this is a conjecture that cannot be proven by the second law of thermodynamics in general. Furthermore, MEP was shown to be equivalent to maximum energy expenditure under certain conditions (e.g. Westhoff and Zehe, 2013). In the context of preferential subsurface flow patterns, this seems to be opposite to the frequently mentioned idea that flow patterns organize in such a way that flow is facilitated most efficiently (McDonnell et al., 2007). In sum it seems that most of the

HESSD
11, 5831–5857, 2014

ideas of optimality in subsurface hydrology, in particular MEP, are still on a visionary level (McDonnell et al., 2007; Westhoff and Zehe, 2013).

In this paper, we transfer the concept of self-organization towards minimum energy expenditure from river networks to subsurface flow patterns. A brief review on the established theory for river networks is presented in the following section, while the more complicated theory for subsurface flow is presented in Sect. 3.

2 The concept of minimum energy expenditure in river networks

Scale-invariant properties of river networks have been known for a long time (Horton, 1945; Hack, 1957), and the idea to relate these properties to minimum energy expenditure (Rodriguez-Iturbe et al., 1992a, b; Rinaldo et al., 1992, 1998) seems to be the first substantial application of optimality principles in hydrology. The basic idea is that river networks organize in such a way that the total energy expenditure of the water on its way through the entire domain is minimized. Energy expenditure is computed from the assumption that the potential energy of the water is dissipated when it flows downslope in a channel, which does not require any deeper knowledge of flow dynamics. The mean energy expenditure (energy per time) of an individual channel segment is

$$P = \rho g q l S \tag{1}$$

where ρ is the density, g the gravitational acceleration, q the mean discharge (volume per time), l the length, and is S the slope of the segment. In order to find those channel networks with the lowest energy expenditure (called optimal channel networks or OCNs), the domain is subdivided into discrete cells exposed to a uniform precipitation. The centers of the cells are linked by channel segments in such a way that each site (except for one or more outlet sites at the boundary) drains to exactly one neighbored site, but can be supplied by an arbitrary subset of its neighbors. This leads to dendritic river networks. The energy expenditure of the entire domain is readily obtained by summing up the contributions of all cells (Eq. 1):

HESSD
11, 5831–5857, 2014

$$P = \rho g \sum_i q_i l_i S_i. \quad (2)$$

The minimization of P has an unrealistic trivial solution consisting of a flat topography where all slopes vanish. This was avoided by considering only networks where the surface is in equilibrium of erosion with a given, homogeneous uplift rate. This means that the idea of an absolute minimum is replaced by a minimization under a given side condition. But in contrast to the energy expenditure itself, computing equilibrium topographies requires a deeper knowledge of the erosion process. The simplest models of fluvial erosion are based on relations of the type

$$S \propto q^{-\theta} \quad (3)$$

with $\theta \approx 0.5$. This relationship was originally found empirically by Hack (1957), but substantiated theoretically later by the so-called stream-power approach (Howard, 1994). In most considerations (including Hack's original work and the work on OCNs), the catchment size is used instead of the discharge q, which makes no difference in case of uniform precipitation in the entire domain.

Inserting Eq. (3) into Eq. (2) leads to

$$P \propto \sum_i l_i q_i^{\gamma} \quad (4)$$

with $\gamma = 1 - \theta \approx 0.5$. This expression allows a minimization of the energy expenditure from the network topology (which determines the discharges or the catchment sizes) alone without explicitly considering the topography. In the studies on OCNs, drainage networks that minimize Eq. (4) (strictly speaking, the version without the term l_i that takes into account the length of the river segments) were determined numerically.

It was found that these OCNs reproduce some well-known statistical properties of real river networks, such as the relationship between river length and catchment size

HESSD
11, 5831–5857, 2014

and the statistical distribution of the catchment sizes, quite well. However, the principle of minimum energy expenditure has never been directly derived from first principle. Later studies using simple erosion models (Hergarten and Neugebauer, 2001; Hergarten, 2002) revealed that some of the statistical properties can be reproduced even a little better for river networks exposed to permanently changing boundary conditions which are clearly above the minimum energy expenditure. So it seems that the principle of minimum energy expenditure in river networks has stayed on the level of a quite well working conjecture.

In the following section we transfer the concept of minimum energy expenditure to subsurface flow. Similarly to river networks, the principle cannot be proven, but remains a conjecture. Afterwards we present two applications to different scenarios and a validation using spring discharge distributions in order to demonstrate that the concept may reach the level of a well working conjecture, too.

3 Theory

In the following, we assume steady-state Darcy flow of an incompressible fluid in an isotropic, but inhomogeneous porous medium with a hydraulic conductivity $K(\boldsymbol{x})$. The volumetric flow rate is then given by

$$\boldsymbol{q}(\boldsymbol{x}) = -K(\boldsymbol{x})\nabla h(\boldsymbol{x}) \tag{5}$$

with the hydraulic potential $h(\boldsymbol{x})$. The total energy expenditure per time for this flow is

$$P = -\rho g \int \boldsymbol{q}(\boldsymbol{x}) \cdot \nabla h(\boldsymbol{x}) \mathrm{d}^3x \tag{6}$$

$$= \rho g \int K(\boldsymbol{x}) |\nabla h(\boldsymbol{x})|^2 \mathrm{d}^3x \tag{7}$$

$$= \rho g \int \frac{q(\boldsymbol{x})^2}{K(\boldsymbol{x})} \mathrm{d}^3x \tag{8}$$

HESSD
11, 5831–5857, 2014

where the integral extends over the considered domain, and $q(\boldsymbol{x}) = |\boldsymbol{q}(\boldsymbol{x})|$.

If the spatial distribution of the conductivity $K(\boldsymbol{x})$ is given, the field $h(\boldsymbol{x})$ which minimizes P is given by the Euler–Lagrange equation of Eq. (7):

$$\frac{\partial}{\partial h(\boldsymbol{x})} P = \operatorname{div} \frac{\partial}{\partial \nabla h(\boldsymbol{x})} P \tag{9}$$

where the derivatives are functional derivatives. This immediately leads to

$$\operatorname{div}(K(\boldsymbol{x}) \nabla h(\boldsymbol{x})) = 0, \tag{10}$$

so that the distribution of $h(\boldsymbol{x})$ which minimizes the energy expenditure automatically satisfies the mass balance as long as there are neither sources nor sinks. Source and sink terms can be included by taking into account the potential energy of the water entering or leaving according to its hydraulic potential. This is the basis of finite-element groundwater modeling.

The key point of this paper is the extension of the principle of minimum energy expenditure towards $K(\boldsymbol{x})$. This means that not only $h(\boldsymbol{x})$ minimizes the energy expenditure (and thus satisfies the mass balance), but the spatial distribution of $K(\boldsymbol{x})$ shall also be optimized with regard to the total energy expenditure. For simplicity and because it is more convenient for application, we determine the optimal spatial distribution of $K(\boldsymbol{x})$ for either $h(\boldsymbol{x})$ given (i.e. minimize Eq. 7) or $q(\boldsymbol{x})$ given (i.e. minimize Eq. 8). In combination with the mass balance (Eq. 10) this is equivalent to finding the optimal combination of $h(\boldsymbol{x})$ and $K(\boldsymbol{x})$ (and thus also $q(\boldsymbol{x})$).

Similarly to the surface drainage network optimization, both problems have trivial solutions, namely $P \to 0$ if $K(\boldsymbol{x}) \to 0$ everywhere ($h(\boldsymbol{x})$ given) or if $K(\boldsymbol{x}) \to \infty$ everywhere ($q(\boldsymbol{x})$ given). We thus need a side condition in analogy to the equilibrium of uplift and erosion for river networks. The idea that the total conductivity, i.e. the conductivity integrated over the entire domain, is given, may be straightforward at first sight. Alternatively, we can assume a given total pore space volume

$$V = \int \phi(\boldsymbol{x}) \mathrm{d}^3 x \tag{11}$$

HESSD
11, 5831–5857, 2014

where $\phi(\boldsymbol{x})$ is the porosity. With respect to preferential flow patterns generated by the flow itself, e.g. in karst systems, the second idea is more suitable because the change in V is the total amount of solid volume that has to be removed (e.g. dissolved).

In order to minimize the energy expenditure under the side condition defined in Eq. (11), the Euler–Lagrange formalism must be applied to the functional $P - \lambda V$ instead of P where the number λ is a Lagrange multiplicator. As neither P nor V contain derivatives of $\phi(\boldsymbol{x})$, the result is formally the same as if ϕ was a parameter instead of a function:

$$\frac{\partial}{\partial\phi(\boldsymbol{x})}P = \lambda\frac{\partial}{\partial\phi(\boldsymbol{x})}V. \tag{12}$$

While the functional derivative at the right-hand size is almost trivial,

$$\frac{\partial}{\partial\phi(\boldsymbol{x})}V(\phi) = 1, \tag{13}$$

computing the left-hand side requires a constitutive law for the conductivity as a function of the porosity, i.e. a function $K(\phi)$.

Relations between porosity and conductivity have been extensively studied since the seminal work of Kozeny (1927) and Carman (1937). The original Kozeny–Carman equation predicts

$$K \propto \frac{\phi^3}{(1-\phi)^2} \tag{14}$$

where the factor of proportionality includes a spatial length scale and the denominator becomes important in case of very high porosities. As the length scale may change if conduits are widened, applying Eq. (14) without further considerations may be misleading. So let us first consider the simple case of parallel tubular conduits of given radii r_i. According to the Hagen–Poiseuille law, the total conductivity of this system is

$$K \propto \sum_i r_i^4, \tag{15}$$

HESSD
11, 5831–5857, 2014

while

$$\phi \propto \sum_i r_i^2. \tag{16}$$

Thus, the increase of conductivity at a given increase of porosity is highest if the largest conduit is widened. In this case we obtain

$$\frac{\partial \log K}{\partial \log \phi} = 2\frac{r_{\max}^2 \sum_i r_i^2}{\sum_i r_i^4} \geq 2, \tag{17}$$

which means that the slope in a double-logarithmic K–ϕ plot is two or larger. It approaches two if either all conduits are equally sized or if the largest conduit is much larger than the rest. So the relationship between conductivity and porosity is not an overall power law, but behaves like a power law with $n = 2$ over some range, while it may increase faster in other regimes. Therefore, an overall power-law relationship

$$K(\phi) = a\,\phi^n \tag{18}$$

with $n \geq 2$ seems to be the best tradeoff between a good approximation and keeping the following considerations as simple as possible. However, most of the results obtained in the following only require $n > 1$, which just means that the conductivity increases more rapidly than the porosity. For simplicity, we neglect the strong increase in conductivity due to the coalescence of conduits for $\phi \to 1$ reflected in the denominator of Eq. (14).

Inserting the expression for the energy expenditure (Eq. 7), the K–ϕ relationship (Eq. 18), and Eq. (13) into Eq. (12) yields

$$\rho g a n \phi(\boldsymbol{x})^{n-1} |\nabla h(\boldsymbol{x})|^2 = \lambda. \tag{19}$$

The Lagrange multiplicator can be eliminated using the total pore space volume V (Eq. 11), leading to

$$\lambda = \rho g a n \left(\frac{V}{\int |\nabla h(\boldsymbol{x})|^{-\frac{2}{n-1}} \mathrm{d}^3 x} \right)^{n-1}, \tag{20}$$

HESSD
11, 5831–5857, 2014

and finally to

$$\phi(\boldsymbol{x}) = V \frac{|\nabla h(\boldsymbol{x})|^{-\frac{2}{n-1}}}{\int |\nabla h(\boldsymbol{\xi})|^{-\frac{2}{n-1}} \mathrm{d}^3\xi}. \tag{21}$$

So the optimal distribution of the porosity if $h(\boldsymbol{x})$ is given is proportional to $|\nabla h(\boldsymbol{x})|^{-\frac{2}{n-1}}$, while the rest of Eq. (21) is just a normalization to maintain the given total pore space volume V.

Minimizing the energy expenditure if $q(\boldsymbol{x})$ is given is similar. Computing the functional derivative of Eq. (8) leads to the condition

$$-\frac{\rho g n q(\boldsymbol{x})^2}{a \phi(\boldsymbol{x})^{n+1}} = \lambda. \tag{22}$$

The Lagrange multiplicator can again be eliminated using the total pore space volume according to

$$\lambda = -\frac{\rho g n}{a} \left(\frac{\int q(\boldsymbol{x})^{\frac{2}{n+1}} \mathrm{d}^3 x}{V} \right)^{n+1}, \tag{23}$$

finally leading to

$$\phi(\boldsymbol{x}) = V \frac{q(\boldsymbol{x})^{\frac{2}{n+1}}}{\int q(\boldsymbol{\xi})^{\frac{2}{n+1}} \mathrm{d}^3\xi}. \tag{24}$$

This dependency is not only similar to that obtained for the case that $h(\boldsymbol{x})$ is given (Eq. 21), but even basically the same. This becomes obvious if we transform Eq. (21) to conductivities, leading to

HESSD
11, 5831–5857, 2014

$$K(\boldsymbol{x}) = aV^n \frac{|\nabla h(\boldsymbol{x})|^{-\frac{2n}{n-1}}}{\left(\int |\nabla h(\boldsymbol{\xi})|^{-\frac{2}{n-1}} \mathrm{d}^3\xi\right)^n} \tag{25}$$

$$\propto |\nabla h(\boldsymbol{x})|^{-\frac{2n}{n-1}}. \tag{26}$$

Applying the same to Eq. (24) leads to

$$K(\boldsymbol{x}) = aV^n \frac{q(\boldsymbol{x})^{\frac{2n}{n+1}}}{\left(\int q(\boldsymbol{\xi})^{\frac{2}{n+1}} \mathrm{d}^3\xi\right)^n} \tag{27}$$

$$\propto q(\boldsymbol{x})^{\frac{2n}{n+1}}. \tag{28}$$

Replacing $q(\boldsymbol{x})$ with $K(\boldsymbol{x})|\nabla h(\boldsymbol{x})|$ in Eq. (28), it is recognized that Eqs. (26) and (28) are equivalent.

Thus, the optimal distribution of porosities and conductivities with respect to minimum energy expenditure is the same for $h(\boldsymbol{x})$ given and for $q(\boldsymbol{x})$ given and can be summarized in the following relations:

$$\phi(\boldsymbol{x}) \propto |\nabla h(\boldsymbol{x})|^{-\frac{2}{n-1}} \propto q(\boldsymbol{x})^{\frac{2}{n+1}} \tag{29}$$

$$K(\boldsymbol{x}) \propto |\nabla h(\boldsymbol{x})|^{-\frac{2n}{n-1}} \propto q(\boldsymbol{x})^{\frac{2n}{n+1}}. \tag{30}$$

In principle, we can now insert this result into the mass balance of Darcy's law and obtain the highly nonlinear differential equation

$$\mathrm{div}\left(|\nabla h(\boldsymbol{x})|^{-\frac{2n}{n-1}} \nabla h(\boldsymbol{x})\right) = 0. \tag{31}$$

However, we should keep in mind that this is a Darcy equation where the conductivity increases even more than linearly with the flow rate. This results in a strong tendency

HESSD
11, 5831–5857, 2014

to focus flow, so that this equation will not have a unique, regular solution in general. For this reason we refrain from considering this equation in detail here.

Beyond this, the resulting optimal distribution of $K(\boldsymbol{x})$ can be used to represent the total energy expenditure as a function of either $h(\boldsymbol{x})$ or $q(\boldsymbol{x})$ alone. Plugging Eq. (25) into Eq. (7) yields

$$P = \frac{\rho g a V^n}{\left(\int |\nabla h(\boldsymbol{x})|^{-\frac{2}{n-1}} \mathrm{d}^3 x\right)^{n-1}}. \tag{32}$$

Thus, minimizing the total energy expenditure is equivalent to maximizing the functional

$$F(h) = \int |\nabla h(\boldsymbol{x})|^{-\frac{2}{n-1}} \mathrm{d}^3 x. \tag{33}$$

It is easily recognized that Eq. (31) is the Euler–Lagrange equation of this functional. As a consequence, maximizing $F(h)$ approximately among a set of functions obeying some regularity should also provide an approximate solution of the nonlinear Darcy flow problem posed in Eq. (31).

An equivalent functional with regard to $q(\boldsymbol{x})$ is obtained by inserting Eq. (27) into Eq. (8), resulting in

$$P = \frac{\rho g}{a V^n} \left(\int q(\boldsymbol{x})^{\frac{2}{n+1}} \mathrm{d}^3 x\right)^{n+1}. \tag{34}$$

Therefore, minimizing P is equivalent to minimizing the functional

$$G(q) = \int q(\boldsymbol{x})^{\frac{2}{n+1}} \mathrm{d}^3 x. \tag{35}$$

This functional will be used in the application presented in Sect. 4.2.

HESSD
11, 5831–5857, 2014

4 Applications

4.1 Radial flow towards a spring

As a simple application we consider radial symmetric flow towards a spring in two dimensions. Due to the two-dimensional structure, K must be interpreted as a transmissivity, i.e. the product of conductivity and thickness, here. An appropriate spatial distribution of the transmissivity has to be assumed when modeling the water fluxes in karstified aquifers without having detailed information on the subsurface structure in the vicinity of springs. If the transmissivity was constant, the hydraulic gradients would strongly increase close to springs, similarly to wells. Therefore, the effective transmissivity (without explicitly considering fractures or karst pipes in the model) must increase towards the spring. The simplest assumption is an increase proportional to $\frac{1}{r}$ (where r is the distance from the point-like spring) that just compensates the decrease of flow cross section towards to spring. This scenario was investigated by Birk and Hergarten (2012).

Let us now determine the optimal distribution of the transmissivity for the radial symmetric case. For a domain of radius R with uniform recharge, the volumetric flow rate is

$$q(r) \propto \frac{R^2 - r^2}{r} \tag{36}$$

as a consequence of the decreasing cross section area. From Eqs. (29) and (30) we immediately obtain

$$\phi(r) \propto \left(\frac{R^2 - r^2}{r} \right)^{\frac{2}{n+1}} \tag{37}$$

$$\propto r^{-\frac{2}{n+1}} \quad \text{for } r \ll R, \tag{38}$$

HESSD
11, 5831–5857, 2014

so that

$$K(r) \propto r^{-\frac{2n}{n+1}} \quad \text{for } r \ll R. \tag{39}$$

This leads to

$$\frac{\partial}{\partial r} h(r) \propto r^{\frac{n-1}{n+1}}, \tag{40}$$

and thus

$$h(r) \propto r^{\frac{2n}{n+1}} \tag{41}$$

close to the spring ($r \ll R$) if $h(0) = 0$. For all values $n > 1$, the predicted increase in $K(r)$ even overcompensates the decrease in cross section area towards the spring, so that the hydraulic gradient even tends to zero when approaching the spring. As discussed in Sect. 3, n should even be at least two in natural aquifers, so that the optimal $K(r)$ should increase at least like $r^{-\frac{4}{3}}$ towards the spring, and $h(r)$ should decrease at least like $r^{\frac{4}{3}}$.

4.2 Dendritic flow patterns

We now come to the direct analog of the optimal channel network approach reviewed in Sect. 2. Similarly to this approach, we focus on two-dimensional flow patterns in plan view. As stated at the end of Sect. 3, minimizing the energy expenditure causes a strong tendency to focus flow, so that an approximation by dendritic networks is appropriate. As a consequence, maze cave structures where flow paths do not only join, but also separate are not optimal in the sense of energy expenditure, similarly to braided rivers.

In analogy to the simulation of river networks we subdivide the domain into square cells where each cell is exposed to the same recharge and assume that each cell drains to one of its eight nearest and second-nearest neighbors. The sole difference between

HESSD
11, 5831–5857, 2014

this approach and two-dimensional Darcy flow is that Darcy's law is only applied in one dimension along the dendritic network, while arbitrary flow directions not necessarily related to a hydraulic gradient are allowed.

For such a discrete network, the functional to be minimized (Eq. 35) turns into that for river networks (Eq. 4) with

$$\gamma = \frac{2}{n+1}. \tag{42}$$

Therefore, the same technique of simulated annealing based on the Metropolis algorithm (Metropolis et al., 1953) can be used for approaching the minimum energy expenditure iteratively. It starts from an arbitrary initial configuration that only has to be consistent in the sense that a flow path from each site to the boundary exists. In each iteration step, the flow direction of a randomly selected site is changed to another (consistent) random direction. If the resulting change in energy expenditure is negative, the change is accepted anyway. However, rejecting all changes where the energy expenditure increases temporarily results in getting stuck at local minima. Therefore, changes which seem to be bad at first sight must be allowed with some probability. During the iteration, the acceptance of changes increasing the energy expenditure is slowly reduced, which can be interpreted as a slow thermodynamic cooling of the system.

Figure 1 shows four realizations on lattices of 4096×4096 sites where outflow is allowed across the entire boundary. As expected, dendritic network structures occur for all values of n considered here. It is easily recognized that focusing flow reduces the total energy expenditure as long as $\gamma < 1$ and thus for all values $n > 1$ according to Eq. (42). As expected, the tendency towards highly branched networks increases with n. Vice versa, some tendency towards the shortest way to the boundary is still visible for $n = 1.5$, in particular when looking at the main drainage divides between the edges of the square. As mentioned above, all reasonable relations between porosity and permeability should have $n \geq 2$ but rather close to two, while the typical value $\gamma = 0.5$ (Eq. 4) corresponds to $n = 3$ according to Eq. (42). Therefore, our model predicts

HESSD
11, 5831–5857, 2014

that the tendency to search the shortest way to the boundary should be slightly stronger for two-dimensional subsurface flow patterns than for rivers at the surface. However, it was already pointed out by Rinaldo et al. (1998) that such small variations in γ do not result in significant differences in the statistical properties of the networks.

As little is known about the internal structure of real subsurface flow patterns, spring discharges provide most easily accessible information. Figure 2 shows that the distribution of the spring discharges Q is a power law described by the probability density

$$f(Q) = Q^{-\tau} \tag{43}$$

with $\tau = 1.5$. Transformed to a cumulative distribution, i.e. the number $N(Q)$ of springs with a discharge greater than or equal to Q, it says

$$N(Q) = Q^{-0.5}. \tag{44}$$

This result is insensitive to n at least in the range $n \geq 1.5$ considered here, and thus for all reasonable relations between porosity and permeability as discussed above.

4.3 Validation

In the following we attempt to validate our model by two data sets of spring discharges from Austria. The first data set comprises the discharges of 1675 springs in the Niedere Tauern Range, and the second one the discharges of 1001 springs in the Semmering region. The methods of data acquisition range from simple estimates to direct capture and tracer dilution techniques. The frequency of measurement also varies from spring to spring. Despite the potential errors in the individual spring discharges, both data sets reveal clear power-law distributions of the discharges above a minimum value of about $0.1\,\mathrm{L\,s^{-1}}$ (Fig. 3). This result suggests that the subsurface flow patterns in the two regions are indeed strongly organized.

Both power-law distributions are strikingly similar even quantitatively. However, the scaling exponent τ appears to be greater than the value $\tau = 1.5$ predicted by the model

HESSD
11, 5831–5857, 2014

(Eq. 43). The estimate $\tau = 1.8$ given in Fig. 3 was determined by visual correlation. Fitting a power-law distribution taking into account the statistical variation in the data reveals a rather high uncertainty in the scaling exponent as determining the minimum discharge where the power law begins is difficult. Starting a power-law fit at a minimum discharge of $0.1\,\mathrm{L\,s^{-1}}$ even yields $\tau < 1.5$, but visually, the data still suggest $\tau > 1.5$ in these two regions.

However, the occurrence of an organized flow pattern does not imply that it is indeed self-organized. And even if it is, it does not proof that this self-organization follows the principle suggested in this study. If the principle of minimizing energy expenditure holds here, the deviations in the scaling exponent may, e.g. arise from a three-dimensional flow organization or from the location of the springs in relation to the topography. On the other hand, the power law distribution might also be the result of a scale-invariant tectonic pre-design and not be related to any self-organization in the flow pattern. Therefore, more datasets are needed to validate or refute our idea of subsurface flow organization.

4.4 Residence time distributions

Residence times and their statistical distributions are among the most important properties in subsurface hydrology. On one hand, they reveal valuable information about storage and flow pathways, and on the other hand they are essential for predicting the propagation of pollutants and recovery.

The spatial distribution of porosity and conductivity has a strong influence on the residence time distribution in a catchment. The residence time distribution is obtained by integrating $\frac{1}{v(\boldsymbol{x})}$ over the flow path from each point of the catchment to the spring. Here,

$$v(\boldsymbol{x}) = \frac{q(\boldsymbol{x})}{\phi(\boldsymbol{x})} \tag{45}$$

denotes the flow velocity. Using Eq. (24) we obtain

HESSD
11, 5831–5857, 2014

$$v(\boldsymbol{x}) = \frac{q(\boldsymbol{x})^{\frac{n-1}{n+1}} \int q(\boldsymbol{\xi})^{\frac{2}{n+1}} \mathrm{d}^3\xi}{V} \tag{46}$$

$$\propto q(\boldsymbol{x})^{\frac{n-1}{n+1}}. \tag{47}$$

Thus, the flow velocity increases with increasing flow rate for all values $n > 1$. However, the increase is weaker than the linear increase occurring in a homogeneous aquifer. The exponent in Eq. (46) amounts to one third for $n = 2$, which means that one third of an increase in flow rate is due to an increase in velocity, while two thirds arise from the increase of conductivity.

At this point it should be mentioned that the residence time distribution obtained this way describes only the contribution of the flow paths since it is assumed that the entire water in a representative volume moves exactly at the velocity defined by Eq. (45). Effects of dispersion and the properties of specific tracers (e.g. sorption) must be taken into account additionally when making a prediction.

The relationship between flow rate and flow velocity is the perhaps most important difference of our model of subsurface flow towards rivers at the surface. Although the theory reviewed in Sect. 2 does not account for flow velocities explicitly, it is clear that the flow velocities of large rivers having a small slope are lower than those of small, but steeper rivers. Therefore, surface rivers show a negative correlation between discharge and velocity in general.

Figure 4 shows the residence time distributions of the examples considered in Sects. 4.1 and 4.2, obtained by evaluating the path integrals over $\frac{1}{v(\boldsymbol{x})}$ according to Eq. (46) numerically. Both geometries yield exponential residence time distributions for a homogeneous aquifer, but completely different distributions otherwise. In the example of radial flow, the distribution changes from being strongly negatively skewed to positively skewed for increasing n. The respective distributions of the dendritic networks are always positively skewed and become more symmetric for increasing n. For $n = 2$

HESSD
11, 5831–5857, 2014

or not much larger which was found to be the most reasonable range, the distributions are moderately positively skewed in both examples.

The residence time distribution for radial flow can be explained directly from Eq. (47) since the flow rate is entirely determined by the recharge and thus independent of n and the same as for a homogeneous aquifer. For small values of n, the increase in velocity towards the spring is much weaker than for in the homogeneous case. As this affects the residence times in the entire catchment, it results in high residence times for large parts of the catchment. In return, velocities approach those of the homogeneous distribution for $n \to \infty$, resulting in a positively skewed residence time distribution.

For the dendritic pattern, the residence time distribution does not only depend on the relationship between flow rate and velocity (Eq. 46), but also on the flow pattern. We therefore have two competing effects of the dendritic structure compared to direct flow towards the boundary. First, the flow length becomes longer for (almost) all sites, but in return, flow in the preferential flow paths is faster. In our example we found that the mean residence times in the dendritic networks are by about 10 % higher than for a homogeneous conductivity. The longest mean residence time was found for $n = 2$, but the dependence on n is rather weak. Notably, the residence time distributions obtained for $n \geq 2$ are similar to those arising from an advection-dispersion model, although the theory behind our model is completely different from this.

5 Conclusions

We have presented a new theoretical concept to derive the properties of subsurface flow patterns from a principle of optimization. In its spirit, the idea is similar to the established idea of minimizing energy expenditure for river networks at the Earth's surface. Due to different physical and empirical laws for surface and subsurface flow, our theory significantly differs from that of surface river networks and is more complicated. Beyond the basic equations, we have to introduce different side conditions for the minimization. While equilibrium between tectonic uplift and erosion is assumed for river networks,

HESSD
11, 5831–5857, 2014

we assume a given total pore space volume and a relationship between porosity and permeability.

Despite the differences in the theories, both concepts finally arrive at basically the same functional to be minimized. As a consequence, the predicted preferential flow patterns in two dimensions are quite similar to surface river networks. The predicted size distribution of the spring discharges follows a power law with a (non-cumulative) scaling exponent $\tau = 1.5$. This result reproduces the spring size distributions of two regions in Austria quite well, although the scaling exponent seems to be slightly higher there, namely $\tau \approx 1.8$. The other application shown in this paper, radial flow towards a spring, makes a suggestion how the permeabilities in the region around a spring might be chosen in a model where preferential flow patterns are not taken into account explicitly.

The residence time distributions seem to be the most striking difference between our model for subsurface flow and rivers at the surface. In contrast to rivers, our theory predicts an increase of flow velocity with flow rate, which is, however, not as strong as in an homogeneous aquifer. As a consequence of the weaker increase, mean residence times are in general higher for optimized flow patterns than for homogeneous aquifers.

Finally it should not be forgotten that, similarly to all other principles of optimization in hydrology, our approach is based on an ad hoc assumption that cannot be directly derived from first principles. The validation based on spring discharge distributions is promising, but not a proof that flow patterns indeed self-organize according to minimum energy expenditure. So further studies are needed in order to investigate the applicability of our hypothesis. These studies will also have to include three-dimensional flow patterns and the influence of external pre-design.

Acknowledgements. This work was funded by the Austrian Science Fund (FWF): L576-N21, the European Regional Development Fund (ERDF), and the Federal Government of Styria. Spring discharge data of the Semmering region were provided by the Austrian Federal Railways ÖBB Infrastruktur AG.

HESSD
11, 5831–5857, 2014

References

Birk, S. and Hergarten, S.: Estimation of aquifer parameters from the recession of spring hydrographs – influence of flow geometry, Geophys. Res. Abstr., 14, EGU2012-9777, 2012. 5843

Carman, P. C.: Fluid flow through granular beds, T. I. Chem. Eng.-Lond., 15, 150–166, 1937. 5838

Dreybrodt, W., Gabrovšek, F., and Romanov, D.: Processes of speleogenesis: a modeling approach, in: Carsologica, vol. 4, ZRC Publishing, Ljubljana, 2005. 5833

Gabrovšek, F. and Dreybrodt, W.: Spreading of tracer plumes through confined telogenetic karst aquifers: a model, J. Hydrol., 409, 20–29, doi:10.1016/j.jhydrol.2011.07.029, 2011. 5833

Groves, C. G. and Howard, A. D.: Early development of karst systems: 1. Preferential flow path enlargement under laminar flow, Water Resour. Res., 30, 2837–2846, doi:10.1029/94WR01303, 1994. 5833

Hack, J. T.: Studies of Longitudinal Profiles in Virginia and Maryland, US Geol. Survey Prof. Papers 294-B, US Government Printing Office, Washington, D.C., 1957. 5834, 5835

Hergarten, S.: Self-Organized Criticality in Earth Systems, Springer, Berlin, Heidelberg, New York, 2002. 5836

Hergarten, S. and Neugebauer, H. J.: Self-organized critical drainage networks, Phys. Rev. Lett., 86, 2689–2692, 2001. 5836

Horton, R. E.: Erosional development of streams and their drainage basins; hydrophysical approach to quantitative morphology, Bull. Geol. Soc. Am., 56, 275–370, 1945. 5834

Howard, A. D.: A detachment-limited model for drainage basin evolution, Water Resour. Res., 30, 2261–2285, 1994. 5835

Howard, A. D. and Groves, C. G.: Early development of karst systems: 2. Turbulent flow, Water Resour. Res., 31, 19–26, doi:10.1029/94WR01964, 1995. 5833

Hubinger, B. and Birk, S.: Influence of initial heterogeneities and recharge limitations on the evolution of aperture distributions in carbonate aquifers, Hydrol. Earth Syst. Sci., 15, 3715–3729, doi:10.5194/hess-15-3715-2011, 2011. 5833

Kaufmann, G. and Braun, J.: Karst aquifer evolution in fractured rocks, Water Resour. Res., 35, 3223–3238, doi:10.1029/1999WR900169, 1999. 5833

Kaufmann, G. and Braun, J.: Karst aquifer evolution in fractured, porous rocks, Water Resour. Res., 36, 1381–1391, doi:10.1029/1999WR900356, 2000. 5833

HESSD
11, 5831–5857, 2014

Kaufmann, G., Romanov, D., and Hiller, T.: Modeling three-dimensional karst aquifer evolution using different matrix-flow contributions, J. Hydrol., 388, 241–250, doi:10.1016/j.jhydrol.2010.05.001, 2010. 5833

Kiraly, L.: Remarques sur le simulation des failles et du réseau karstique par élèments finis dans les modelès d'écoulement, Bull. Centre Hydrogéol., 3, 155–167, 1979. 5833

Kleidon, A. and Schymanski, S. J.: Thermodynamics and optimality of the water budget on land: a review, Geophys. Res. Lett., 35, L20404, doi:10.1029/2008GL035393, 2008. 5833

Kozeny, J.: Über kapillare Leitung des Wassers im Boden, Sitzungsber. Akad. Wiss. Wien, 136, 271–306, 1927. 5838

Liedl, R., Sauter, M., Hückinghaus, D., Clemens, T., and Teutsch, G.: Simulation of the development of karst aquifers using a coupled continuum pipe flow model, Water Resour. Res., 39, 1057, doi:10.1029/2001WR001206, 2003. 5833

McDonnell, J. J., Sivapalan, M., Vaché, K., Dunn, S., Grant, G., Haggerty, R., Hinz, C., Hooper, R., Kirchner, J., Roderick, M. L., Selker, J., and Weiler, M.: Moving beyond heterogeneity and process complexity: a new vision for watershed hydrology, Water Resour. Res., 42, W07301, doi:10.1029/2006WR005467, 2007. 5833, 5834

Metropolis, N., Rosenbluth, A. W., Rosenbluth, M. N., Teller, A. H., and Teller, E.: Equation of state calculations by fast computing machines, J. Chem. Phys., 21, 1087–1092, doi:10.1063/1.1699114, 1953. 5845

Rinaldo, A., Rodriguez-Iturbe, I., Bras, R. L., Ijjasz-Vasquez, E., and Marani, A.: Minimum energy and fractal structures of drainage networks, Water Resour. Res., 28, 2181–2195, 1992. 5833, 5834

Rinaldo, A., Rodriguez-Iturbe, I., and Rigon, R.: Channel networks, Annu. Rev. Earth Pl. Sc., 26, 289–327, 1998. 5834, 5846

Rodriguez-Iturbe, I., Rinaldo, A., Rigon, R., Bras, R. L., Ijjasz-Vasquez, E., and Marani, A.: Fractal structures as least energy patterns: the case of river networks, Geophys. Res. Lett., 19, 889–892, doi:10.1029/92GL00938, 1992a. 5833, 5834

Rodriguez-Iturbe, I., Rinaldo, A., Rigon, R., Bras, R. L., Marani, A., and Ijjasz-Vasquez, E.: Energy dissipation, runoff production, and the three-dimensional structure of river basins, Water Resour. Res., 28, 1095–1103, 1992b. 5833, 5834

Siemers, J. and Dreybrodt, W.: Early development of Karst aquifers on percolation networks of fractures in limestone, Water Resour. Res., 34, 409–419, doi:10.1029/97WR03218, 1998. 5833

HESSD
11, 5831–5857, 2014

Westhoff, M. C. and Zehe, E.: Maximum entropy production: can it be used to constrain conceptual hydrological models?, Hydrol. Earth Syst. Sci., 17, 3141–3157, doi:10.5194/hess-17-3141-2013, 2013. 5833, 5834

HESSD
11, 5831–5857, 2014

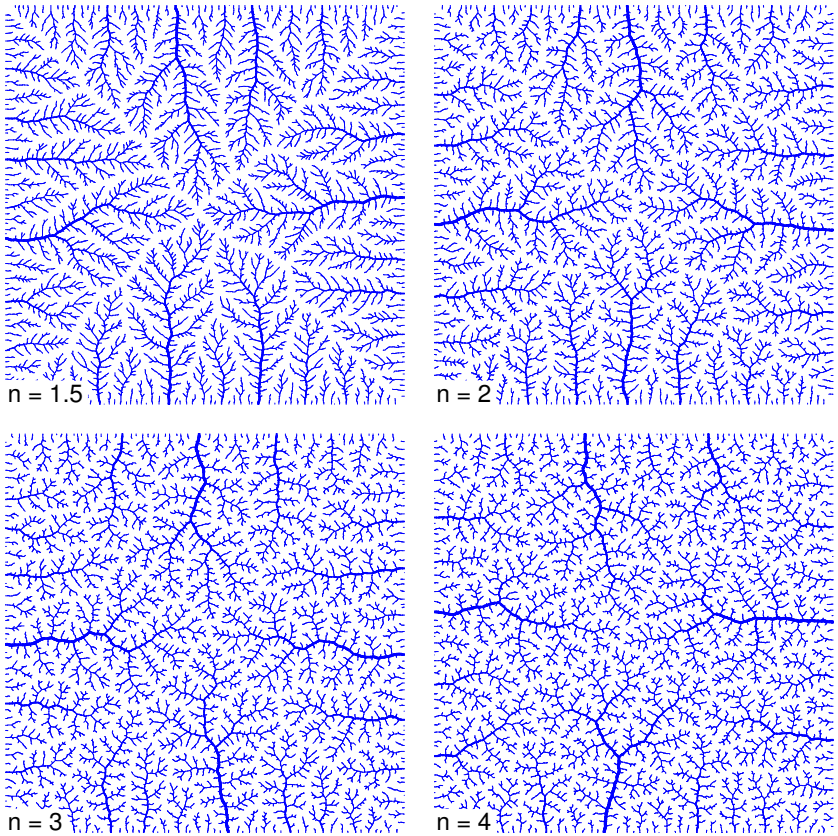

Figure 1. Dendritic flow patterns obtained by numerical optimization for different values of n on lattices of 4096 × 4096 sites. Only flow paths with a discharge of at least 10^{-5} of the total recharge are plotted. The line width is proportional to the third root of the discharge, which is proportional to the diameter of the conduits for $n = 2$.

HESSD
11, 5831–5857, 2014

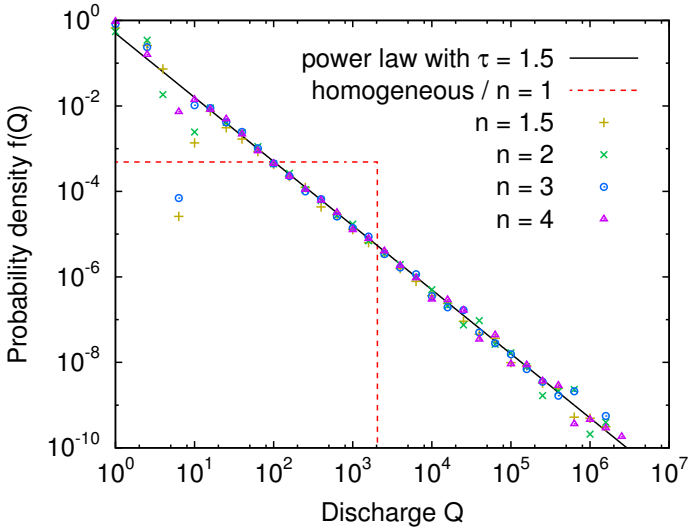

Figure 2. Probability density of the spring discharges of the flow patterns shown in Fig. 1 measured along the boundaries of the domain. Discharges are scaled by assuming a unit recharge at each site, so that the discharge is the same as the number of sites in the respective catchment. The estimated discrete values were obtained by logarithmic binning with five bins per decade. The distributions for homogeneous porosity and for $n = 1$ are identical and correspond to straight flow lines towards the boundary.

HESSD
11, 5831–5857, 2014

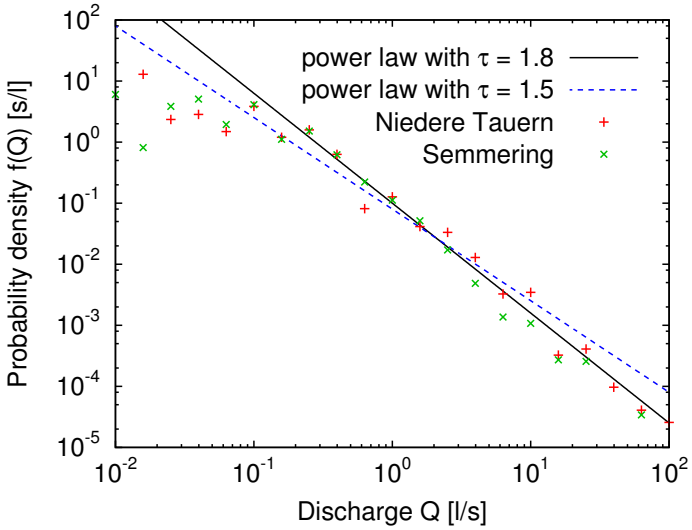

Figure 3. Probability density of the spring discharges of the two considered data sets from Austria. The estimated discrete values were obtained by logarithmic binning with five bins per decade.

HESSD
11, 5831–5857, 2014

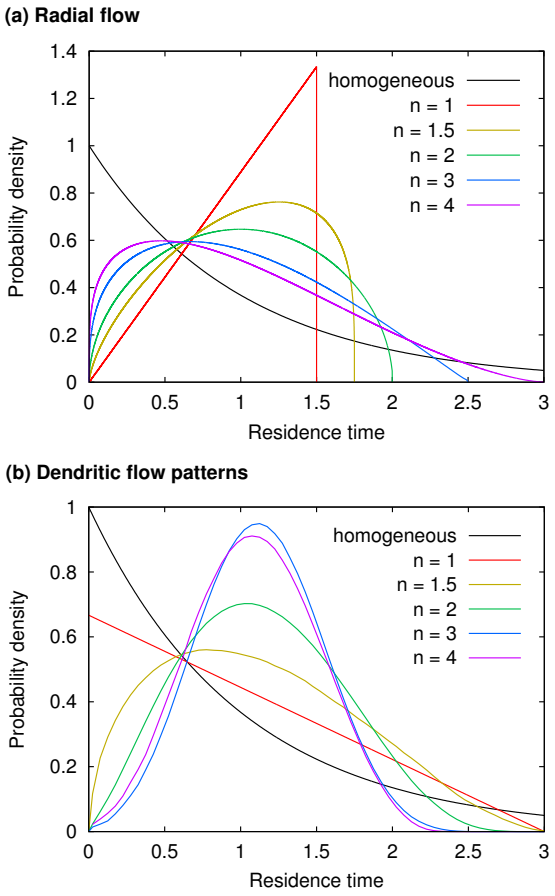

Figure 4. Residence time distributions for the two examples considered in Sects. 4.1 **(a)** and 4.2 **(b)**. The nondimensional time axis is scaled in such a way that the mean residence time is one for the homogeneous distribution of the conductivity, and the total pore space volume is the same in all cases.

HESSD
11, 5831–5857, 2014